This is a repository copy of *A precise measurement of the magnetic field in the corona of the black hole binary V404 Cygni*.

White Rose Research Online URL for this paper:
http://eprints.whiterose.ac.uk/125990/

Version: Accepted Version

Title: A Precise Magnetic Field Measurement in the Corona of the Black Hole Binary V404 Cygni

Authors: Yigit Dallilar[1,★], Stephen S. Eikenberry[1], Alan Garner[1], Richard D. Stelter[1], Amy Gottlieb[1], Poshak Gandhi[2], Piergiorgio Casella[3], Vik S. Dhillon[4,5], Tom R. Marsh[6], Stuart P. Littlefair[4], Liam Hardy[4], Rob Fender[7], Kunal Mooley[7], Dominic J. Walton[8], Felix Fuerst[9,10], Matteo Bachetti[11], Miguel Charcos[1], Michelle L. Edwards[12], Nestor M. Lasso- Cabrera[13], Antonio Marin-Franch[13], S. Nicholas Raines[1], Kendall Ackley[1], John G. Bennett[1], A. Javier Cenarro[13], Brian Chinn[1], H. Veronica Donoso[1], Raymond Frommeyer[1], Kevin Hanna[1], Michael D. Herlevich[1], Jeff Julian[1], Paola Miller[1], Scott Mullin[1], Charles H. Murphey[1], Chris Packham[14,15], Frank Varosi[1], Claudia Vega[1], Craig Warner[1], A.N. Ramaprakash[16], Mahesh Burse[16], Sujit Punnadi[16], Pravin Chordia[16], Andreas Gerarts[17], Héctor de Paz Martín[17], María Martín Calero[17], Riccardo Scarpa[5,17], Sergio Fernandez Acosta[17], William Miguel Hernández Sánchez[17], Benjamin Siegel[17], Francisco Francisco Pérez[17], Himar D. Viera Martín[17], José A. Rodríguez Losada[17], Agustín Nuñez[17], Álvaro Tejero[17], Carlos E. Martín González[17], César Cabrera Rodríguez[17], Jordi Molgó[17], J. Esteban Rodriguez[17], J. Israel Fernández Cáceres[17], Luis A. Rodríguez García[17], Manuel Huertas Lopez[17], Raul Dominguez[17], Tim Gaggstatter[17], Antonio Cabrera Lavers[17], Stefan Geier[5,17], Peter Pessev[5,17], Ata Sarajedini[1], A.J. Castro-Tirado[18,19]

Affiliations:

[1]Department of Astronomy, University of Florida, 211 Bryant Space Science Center, Gainesville, FL 32611, USA.

[2]Department of Physics and Astronomy, University of Southampton, Highfield, Southampton SO17 1BJ, UK.

[3]INAF-Osservatorio Astronomico di Roma, Via Frascati 33, I-00040 Monteporzio Catone, Italy.

[4]Department of Physics and Astronomy, University of Sheffield, Sheffield S3 7RH, UK.

[5]Instituto de Astrofisica de Canarias, 38205 La Laguna, Santa Cruz de Tenerife, Spain.

[6]Department of Physics, University of Warwick, Gibbet Hill Road, Coventry, CV4 7AL, UK.

[7]Astrophysics, Department of Physics, University of Oxford, Keble Road, Oxford OX1 3RH, UK.

[8]Institute of Astronomy, University of Cambridge, Madingley Road, Cambridge CB3 0HA, UK.

[9]Space Radiation Laboratory, California Institute of Technology, Pasadena, CA 91125, USA.

[10]European Space Astronomy Centre (ESA/ESAC), Operations Department, Villanueva de la Cañada (Madrid), Spain.

[11]INAF-Osservatorio Astronomico di Cagliari, via della Scienza 5, 09047 Selargius, Italy.

[12]LBT Observatory, University of Arizona, 933 N. Cherry Ave, Tucson, AZ 85721, USA.

[13]Centro de Estudios de Física del Cosmos de Aragón. 44001 Teruel, Aragón, Spain.

[14]University of Texas at San Antonio. Department of Physics and Astronomy. One UTSA Circle, San Antonio, TX 78249, USA.

[15]National Astronomical Observatory of Japan. 2-21-1 Osawa Mitaka Tokyo, 181-8588, Japan.

[16]Inter-University Center for Astronomy and Astrophysics, Post Bag 4, Ganeshkhind, Pune-411007, India.

[17]GRANTECAN, Cuesta de San José s/n, E-38712, Breña Baja, La Palma, Spain.

[18]Instituto de Astrofísica de Andalucía (IAA-CSIC), P.O. Box 03004, E-18008 Granada, Spain.

[19]Unidad Asociada Departamento de Ingeniería de Sistemas y Automática, Universidad de Málaga, 29071 Malaga, Spain.

Abstract: Observations of black hole and neutron star accreting binaries often show X-ray emission extending to high energies (>10 keV) ascribed to an accretion disk "corona" of energetic particles akin to those seen in the solar corona. Despite their importance and ubiquity, the physical conditions in accretion disk coronae remain poorly constrained. Using simultaneous infrared, optical, X-ray, and radio observations during a rapid synchrotron cooling event in its 2015 outburst, we present a precise 461±12 Gauss magnetic field measurement in the corona of the Galactic black hole system V404 Cygni. This first high-precision measurement of the magnetic field in such a system is significantly lower than previous estimates, providing key constraints for detailed physical models of accretion physics in black hole and neutron star binary systems.

One Sentence Summary: We measure a magnetic field of 461±12 Gauss in the accretion disk corona of V404 Cygni - substantially lower than previous estimates and assumptions.

Main Text: Accretion disk coronae (ADC) are thought to play an important role in compact object accretion flows and energetics, with an especially critical role in black holes that show relativistic jet outflows. Theory predicts that the thick geometry of the ADC leads to the magnetic field configuration needed to power jet outflows, and spectral models show that the jet base is identical to the corona in these systems. (1,2,3) However, until now we have very poor constraints on the detailed physical conditions in the jet-launching coronae. The black hole transient source V404 Cygni was discovered in 1989(4), and subsequent observations revealed a black hole of 9-10 $M_\odot$ in a 6.5(d) binary(5) with a 0.7 $M_\odot$ KIII companion at a distance of 2.39 kpc(6). The system produced a brief X-ray outburst starting on June 15th, 2015(7,8) which lasted about two weeks, exhibiting complex behavior including: (i) complicated X-ray emission dissimilar to the common hard/soft states in black hole binaries including occasional bright flares (9,10); (ii) Long-term correlations in the optical and X-ray lightcurves attributed by previous authors to thermal X-ray reprocessing(11); (iii) Fast (<1s) red optical flares indicating optically thin synchrotron emission from compact regions probably located in a relativistic jet outflow(12); (iv) variable polarization flares indicative of shocks propagating through a relativistic jet outflow(13); (v) X-ray/radio correlations consistent with jet activity(14).

We present multi-wavelength observations taken on June 25th, 2015 in Fig. 1, including near-infrared observations with the Canarias Infrared Camera Experiment (CIRCE) on the 10.4-meter Gran Telescopio Canarias(15), three-band optical observations with ULTRACAM(12,16) on the 4.2-meter William Herschel Telescope, X-ray observations from the NuSTAR satellite(17,18), and three-band GHz radio observations with the AMI telescope(19) - one day after the jet-induced polarization flare observations(13). The radio, optical/infrared(OIR), and X-ray bands exhibit quasi-independent behaviors. The CIRCE lightcurve resembles the ULTRACAM optical

lightcurves, including slow modulations of a few minutes with occasional fast flares (which match the jet-related fast flares seen the following day(12)). The OIR flux levels are >50x higher than the quiescent flux from V404 Cygni in the 2MASS catalog, indicating that the mass donor star contributes little light, and the emission here is dominated by outburst-related processes. The radio emission rises smoothly to 150 mJy - an increase of ~x10 over ~1 hr, also indicating jet activity(14). The complex X-ray lightcurve shows two episodes of enhanced X-ray activity coincident with slow modulations in the OIR lightcurves, as noted in previous studies of this outburst(9,11). However, other slow OIR modulations exhibit no strong X-ray activity, indicating that the origin of the slow modulations must be more complex than a simple X-ray reprocessing scenario.

Here we focus on a selected time interval just before 57198.23 MJD (at t~68 minutes in Fig.1), which covers a sudden flux decay in all bands from infrared to X-ray. This decay comes at the end of a ~30-min episode of bright, slowly-varying OIR emission accompanied by several rapid X-ray flares. During 4 days of ULTRACAM observations of V404 Cygni around this time, this is the only such decay event, so it clearly differs from the rest of the observations (see Fig.12, 12). In Fig.2, we zoom into this selected time interval, with the OIR lightcurves normalized to pre-event fluxes. We model the flux profiles with an exponential decay function (Fig.2; Table 1), whose characteristic timescale (τ) puts an upper limit on the size of the emitting region, via causality and time-of-flight arguments, of $R < 1.25\ c\tau$(20). We note that this approach provides a firm upper limit to the ADC size, allowing considerably smaller values consistent with published results(12).

To compare with a possible thermal blackbody origin for the flux during this event, we take the observed color temperature from the ratio of g' and r' bands and calculate an expected thermal emission region size. We find that the required thermal emission region size is too large (by >x2) to match the observed variability timescale, and we can reject the thermal-dominant emission hypothesis with a confidence >5σ (see Fig.S1). This effectively eliminates blackbody emission processes (including X-ray reprocessing on the accretion disk or companion star(11)) as possible origins for the primary OIR emission during the event, and indicates that a non-thermal emission process (i.e. synchrotron or Compton scattering) must be the dominant source of the OIR flux. There is a small OIR "flare" at the top of the lightcurve just prior to the cooling event, which slightly lags the peak of the X-ray, and may be a low-amplitude X-ray reprocessing signature or an internal shock in a relativistic jet outflow (see Fig.S2).

The best fit power-law function to $\tau(v)$ for the data in Table 1 reveals the relation $\tau \propto v^{-0.49\pm0.03}$ where v is the observed frequency of the radiation and τ represents the decay timescale in each band during the cooling event in Fig. 2(20). This result is in excellent agreement with the relation ($\tau \propto v^{-1/2}$) (unique to synchrotron cooling processes) over five order of magnitude in frequency(Fig. 3). We eliminate Compton cooling as the origin of the cooling curve in the OIR band, based on the magnetic to photon energy densities(20). While we cannot strictly eliminate Compton cooling for the X-rays, we note that while thermal or Compton processes could possibly emulate this $v^{-1/2}$ frequency scaling, there is no a priori reason to expect them to do so, especially over such a large frequency range. This seems to confirm our conclusion that synchrotron processes appear most likely to dominate this event. However, we find, with marginal significance, slightly slower cooling timescales in hard (10-79 keV) versus soft 3-10 keV) X-rays, so we cannot reject a possible contribution from Comptonization processes here.

In Table 1, we calculate individual synchrotron cooling magnetic field measurements from these timescales, obtaining a best-fit mean magnetic field(B_0) value of 461±12 Gauss with reduced $\chi^2_\nu = 0.8$. The individual magnetic field values are all consistent with the mean value within their ~1σ uncertainties (which are all <26%, and some as small as 2%). The fact that a simple single-zone magnetic field model fits all bands simultaneously over 5 decades in energy for a time-coincident event implies that the dominant emission for this event is consistent with an origin from a single population of electrons with a common magnetic field. The derived magnetic field is the first measurement in an accreting black hole system with this precision - the fractional uncertainties are 25x smaller than those for jet magnetic field strength in GX339-4[21] (which were themselves unprecedented in their precision at the time). We also note that there is no apparent variation in the magnetic field strength during the event, from a decay timescale of <2 seconds in X-rays to >100s in the OIR. We estimate a maximum fractional change in the magnetic field of $\Delta B / B_0 < 15\%$[20]. We can use this constraint to investigate possible expansion of the synchrotron-emitting region (i.e. due to expansion in a relativistic jet outflow). Magnetic field conservation arguments for adiabatically expanding synchrotron plasmoids generally lead to the conditions, $B \propto R^{-\alpha}$, with $1 < \alpha < 2$ and R as radius of synchrotron source[22]. For the limiting case $\alpha = 1$, any fractional variation in the emitting region size is thus limited to $\Delta R / R < 15\%$. This upper limit suggests a stationary and stable region for the origin of the radiation – a stationary cloud of high energy electrons confined to a small region, which is the expected disk corona structure for accreting black hole binaries, as opposed to discrete ejections expanding and moving with relativistic velocities[23].

Minimum energy requirements for synchrotron sources have been used to estimate "equipartition" magnetic field strengths in extragalactic and Galactic accreting black hole systems. Although there are some well-known caveats to this approach[24], recent studies have demonstrated evidence for charged particle energies being in equilibrium with the magnetic field energy in a jet system[25]. Applying these arguments to the V404 Cygni cooling event, we derive an equipartition magnetic field strength of $B_{eq} = 651 \, k^{2/7} (F_\nu / 1 \text{ Jy})^{2/7} (\nu / 10^{15} \text{ Hz})^{1/7} (\tau / 2 \text{ sec})^{-6/7}$ Gauss[20], where k is defined to be the energy ratio of all charged particles to low-mass charged particles (electrons and positrons) in the system. The k factor is expected to be >1 for environments with relativistic bulk motions in which the mechanical energy of high-mass charged particles (protons or ions) can dominate the energy of low-mass charged particles. As there is no clear evidence of bulk motions during the decay of the OIR flux since, we assume k ~1. The derived equipartition field strength of ~650 G is thus very close to the measured value of 461G we present here, indicating that during this event V404 Cygni was near to an equipartition energy configuration. We then can derive the energetics in the system: magnetic field energy $U_B = V u_B \sim 7.4 \times 10^{36} (\tau / 2 \text{ sec})^3$ ergs, electron kinetic energy $U_e = V u_e \sim 2.2 \times 10^{37} (F_\nu / 1 \text{ Jy})(\nu / 10^{15} \text{ Hz})^{1/2}$ ergs, and the total energy $U_{\text{tot}} = U_B + U_e \sim 3 \times 10^{37}$ ergs[20]. Here, V represents the emitting volume, and u_B and u_e are the magnetic field and electron energy densities respectively. During our observations, the OIR luminosities reach ~10^{37} ergs/s, indicating that the overall energy budget of the corona is comparable to ~1s (or less) of the system luminosity - consistent with the rapid variations observed during this outburst being tied to and powered by variations in the accretion luminosity.

We present the overall spectral energy distribution at the start of the synchrotron cooling event in Fig.4, along with the corresponding electron energies/densities separately given in Fig.S3. In

the OIR, we show only the excess flux above the post-decay level (since thermal processes might be dominant in the remaining flux(20)). The electron Lorentz factors range from $\gamma \sim$2-3 for the radio to $\gamma \sim 10^2$–10^3 for the OIR bands and $\gamma \sim 10^5$ for the X-ray emission - covering the range from mildly relativistic to fully relativistic electrons. The overall distribution at the start of the event is the product of the history of relativistic electron injection into the coronal region at various times during the preceding activity in V404 Cygni, convolved with the relevant energy-dependent cooling timescales. We have no direct insight into the magnetic field properties during this time, nor into the acceleration mechanism populating the corona with relativistic electrons. However, if we assume that the cooling timescales (and thus magnetic field strengths) resemble those measured in the cooling event itself, we can infer possible scenarios. In particular, the X-ray cooling timescales (and associated X-ray emitting lifetimes of the electrons) would be very short ($\sim$2 seconds), so that the X-ray lightcurve variability would imply multiple electron acceleration/injection episodes over this period, each lasting several minutes and with significant substructure. The observed correlation of the OIR flux with these events shows smoother OIR variability (as expected for longer-timescale synchrotron cooling of lower-energy electrons). The observed correlations are not necessarily one-to-one between the OIR and X-rays, possibly implying a variable electron energy spectrum at the acceleration site. Given the complex lightcurve "history", multiple breaks in the flux distribution (and inferred electron energy distribution) at the start of the fading event would arise naturally, (see Fig.4 and Fig.S3). For instance, the X-ray spectral/energy distribution does not connect smoothly with the OIR region. Again, this is consistent with the much shorter synchrotron timescale for the X-ray emitting electrons (and thus shorter effective "memory" of the system) compared to the typical injection episode spacings of 10-100s, which are comparable to or shorter than the expected OIR synchrotron cooling timescales. There is another break between the OIR and radio emission, as commonly seen in black hole binaries, and usually interpreted as rising synchrotron self-absorbed emission from a "radio photosphere" with $R \sim 10^{12}$- 10^{13} cm(20) containing low-energy electrons and corresponding light-crossing times of hundreds of seconds and possibly tied to a large-scale jet feature. This matches both the observed smoothness of the radio lightcurve and the expected synchrotron opacity at these electron energies/densities for the measured field strength. The OIR emission is expected to be optically thin, and thus on the other side of this opacity-induced break.

This precise magnetic field value provides important constraints for jet launching/emission models, especially since it is much lower than previous estimates for other sources: $\sim 10^5$-10^7 G (Cyg X-1(26)), $\sim 5 \times 10^4$ G (XTE J1550-564(27)), and the most precise previous measurement of $1.5(\pm 0.8) \times 10^4$ (GX339-4(21)). This lower field would tend to shift the model electron energy distribution to higher Lorentz factors (by x30 or more), and significantly alter the size of the emitting region, the particle density, and the overall energy budget of the corona. Furthermore, previous studies follow a scaling between inferred magnetic field and a spectral break frequency in the SED of $B \sim \upsilon_b L^{-1/9}$(27,28). If we associate the OIR peak in Fig. 4 with this break and scale from GX339-4, we would expect $B \sim 2 \times 10^4$ G for V404 Cygni - off by $\sim$400x, indicating that the scaling relation may not hold as broadly or simply as previously thought. However, the decay event here only reveals the physical conditions in the jet-launching corona at the time when electron injection/acceleration stops. We have no direct information regarding the "accelerator" creating the electron population in the first place. A non-expanding emission region somehow physically distinct from the acceleration region in V404 Cygni (and not

previously seen in the other sources) could also explain the scaling difference, albeit while requiring a theory of varying jet base structure between sources.

References and Notes:

1. D. L. Meier, The association of jet production with geometrically thick accretion flows and black hole rotation. Astrophys. J Lett. **548**, L9-12 (2001).

2. S. Markoff, H. Falcke, R. Fender, A jet model for the broadband spectrum of XTE J1118+480. Synchrotron emission from radio to X-rays in the Low/Hard spectral state. Astron. Astrophys. **372**, 25-28 (2001).

3. S. Markoff et al., Exploring the role of jets in the radio/X-ray correlations of GX 339-4. Astron. Astrophys. **397**, 645-658 (2003).

4. F. Makino, GS 2023+338. IAU Circ. **4782** (1989).

5. J. Casares et al., Optical studies of V404 Cyg, the X-ray transient GS2023+338. I. The 1989 outburst and decline. Mon. Not. R. Astron. Soc. **250**, 712–725 (1991).

6. J. C. A. Miller-Jones et al., The first accurate parallax distance to a black hole. Astrophys. J. **706**, L230–L234 (2009).

7. S. D. Barthelmy, A. D'ai, P. D'avanzo, Swift trigger 643949 is V404 Cyg. GCN Circ (2015).

8. H. Negoro et al., MAXI/GSC detection of a new outburst from the Galactic black hole candidate GS 2023+338 (V* V404 Cyg). The *Astronomer's* Telegram. **7646** (2015).

9. J. Rodriguez et al., Correlated optical, X-ray, and γ-ray flaring activity seen with INTEGRAL during the 2015 outburst of V404 Cygni. Astron. Astrophys. **581**, L9 (2015).

10. T. M. Belloni, "States and transitions in black hole binaries" in The Jet Paradigm: From Microquasars to Quasars (Springer-Verlag, Berlin, 2010).

11. M. Kimura et al., Repetitive patterns in rapid optical variations in the nearby black-hole binary V404 Cygni. Nature. **529**, 54–58 (2016).

12. P. Gandhi et al., Furiously fast and red: sub-second optical flaring in V404 Cyg during the 2015 outburst peak. Mon. Not. R. Astron. Soc. **459**, 554–572 (2016).

13. T. Shahbaz et al., Evidence for magnetic field compression in shocks within the jet of V404 Cyg. Mon. Not. R. Astron. Soc. **463**, 1822-1830 (2017).

14. R. M. Plotkin et al., The 2015 decay of the black hole X-Ray binary V404 Cygni: Robust disk-jet coupling and a sharp transition into quiescence. Astrophys. J. **834**, 104 (2017).

15. S. S. Eikenberry et al., Journal of Astronomical Instrumentation, submitted.

16. V. S. Dhillon et al., ULTRACAM: an ultrafast, triple-beam CCD camera for high-speed astrophysics. Mon. Not. R. Astron. Soc. **378**, 825-840 (2007).

17. F. A. Harrison et al., The Nuclear Spectroscopic Telescope Array (NuSTAR) high energy Xray mission. Astrophys J. **770**, 103 (2013).

18. D. Walton et al., Astrophys. J., in press (available at https://arxiv.org/abs/1609.01293).

19. J. T. L. Zwart et al., The Arcminute Microkelvin Imager. Mon. Not. R. Astron. Soc. **391**, 1545-1558 (2008).

20. Materials and methods are available as supplementary materials at the Science website.

21. P. Gandhi et al., A variable mid-infrared synchrotron break associated with the compact jet in GX 339-4. Astrophys. J. Lett. **740**, L13 (2011).

22. H. C. Spruit, F. Daigne, G. Drenkhahn, Large scale magnetic fields and their dissipation in GRB fireballs. Astron. Astrophys. **369**, 694–705 (2001).

23. R. Fender, "'Disc-Jet' coupling in black hole X-ray binaries and active galactic nuclei" in The Jet Paradigm: From Microquasars to Quasars (Springer-Verlag, Berlin, 2010).

24. A. A. Zdziarski, The minimum jet power and equipartition. Mon. Not. R. Astron. Soc. **445**, 1321–1330 (2014).

25. L. Stawarz et al., Giant lobes of Centaurus A radio galaxy observed with the Suzaku X-Ray Satellite. Astrophys. J. **766**, 48 (2013).

26. M. Del Santo, The magnetic field in the X-ray corona of Cygnus X-1. Mon. Not. R. Astron. Soc. **430**, 209–220 (2013).

27. S. Chaty, G. Dubus, A. Raichoor, Near-infrared jet emission in the microquasar XTE J1550-564. Astron. Astrophys. **529**, A3 (2011).

28. D. M. Russell et al., Jet spectral breaks in black hole X-ray binaries. Mon. Not. R. Astron. Soc. **429**, 815-832 (2013).
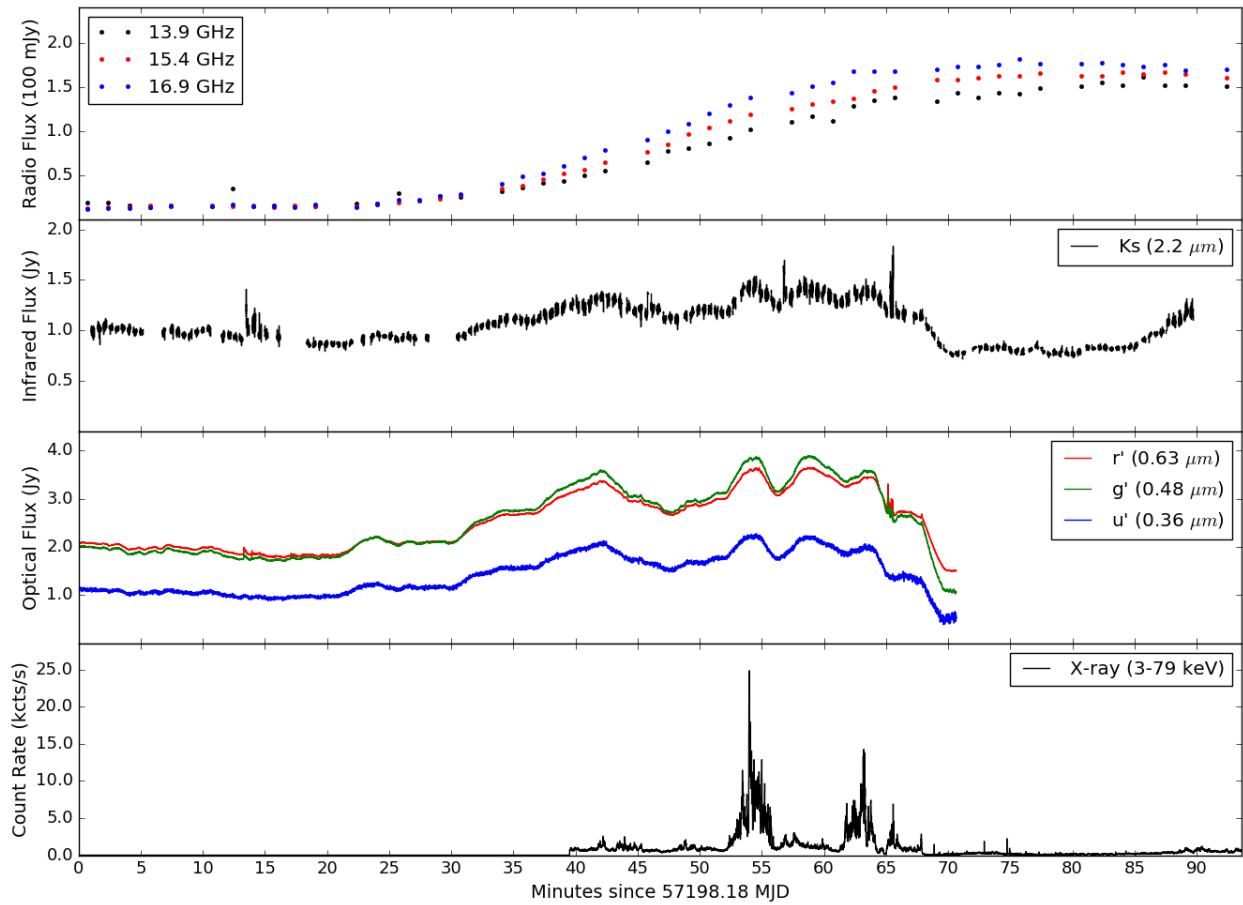
Fig. 1. **Multi-wavelength (radio, near-infrared, optical, and X-ray) lightcurves of V404 Cygni on MJD 57198 during the 2015 outburst.** The OIR flux shows slow modulations punctuated by fast red flares. The two OIR "bumps" at ~54 and ~63 minutes correlate with bright X-ray flares, while the OIR bumps at ~42 and ~58 minutes shows very little (if any) X-ray activity, indicating that models invoking simple X-ray reprocessing are unlikely to fit. The cooling event is at ~68 minutes.
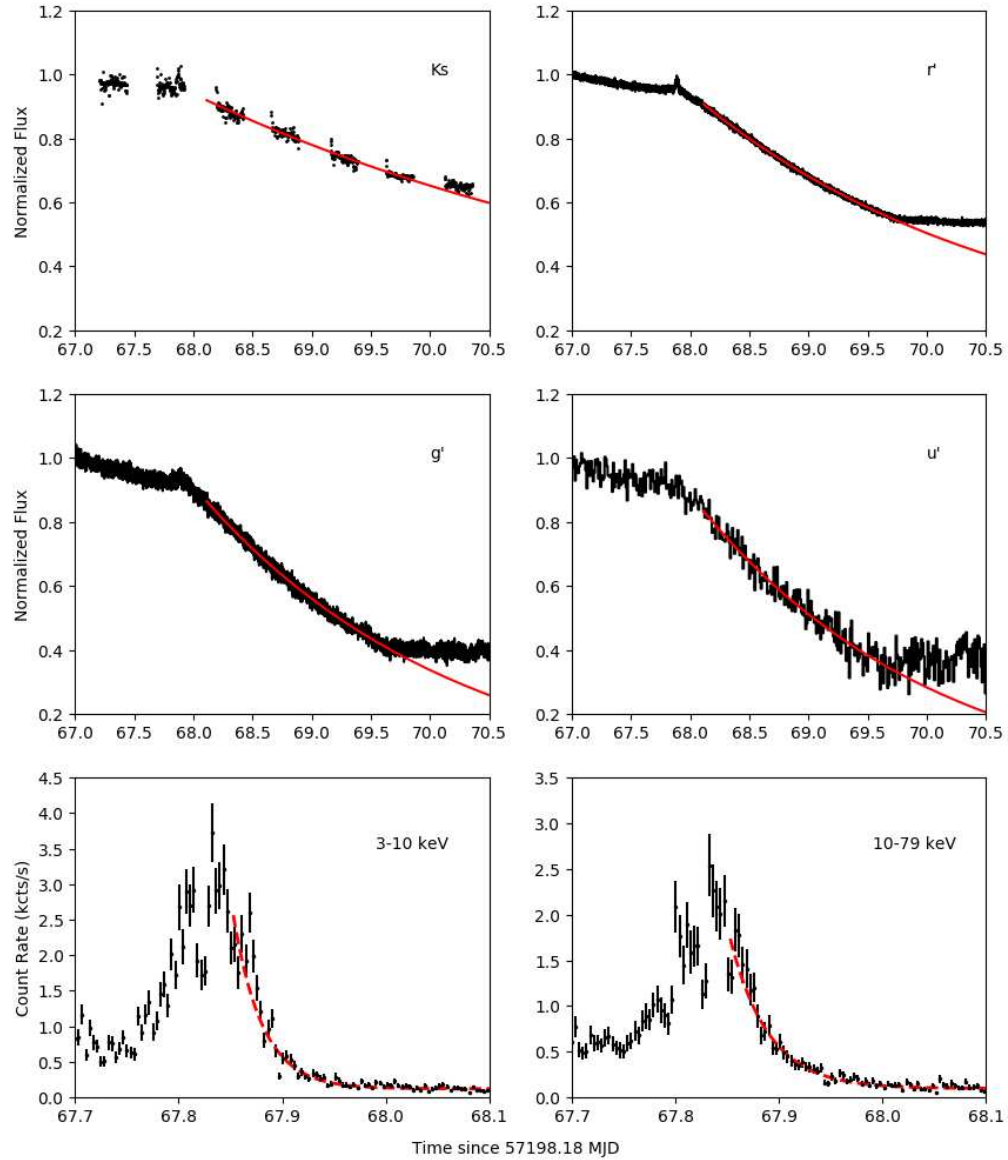
Fig. 2. Simultaneous cooling event decay curves with best-fit exponential models. Black lines represent the data and red lines the best-fit exponential decay profile for the six different energy bands (see also Table 1).
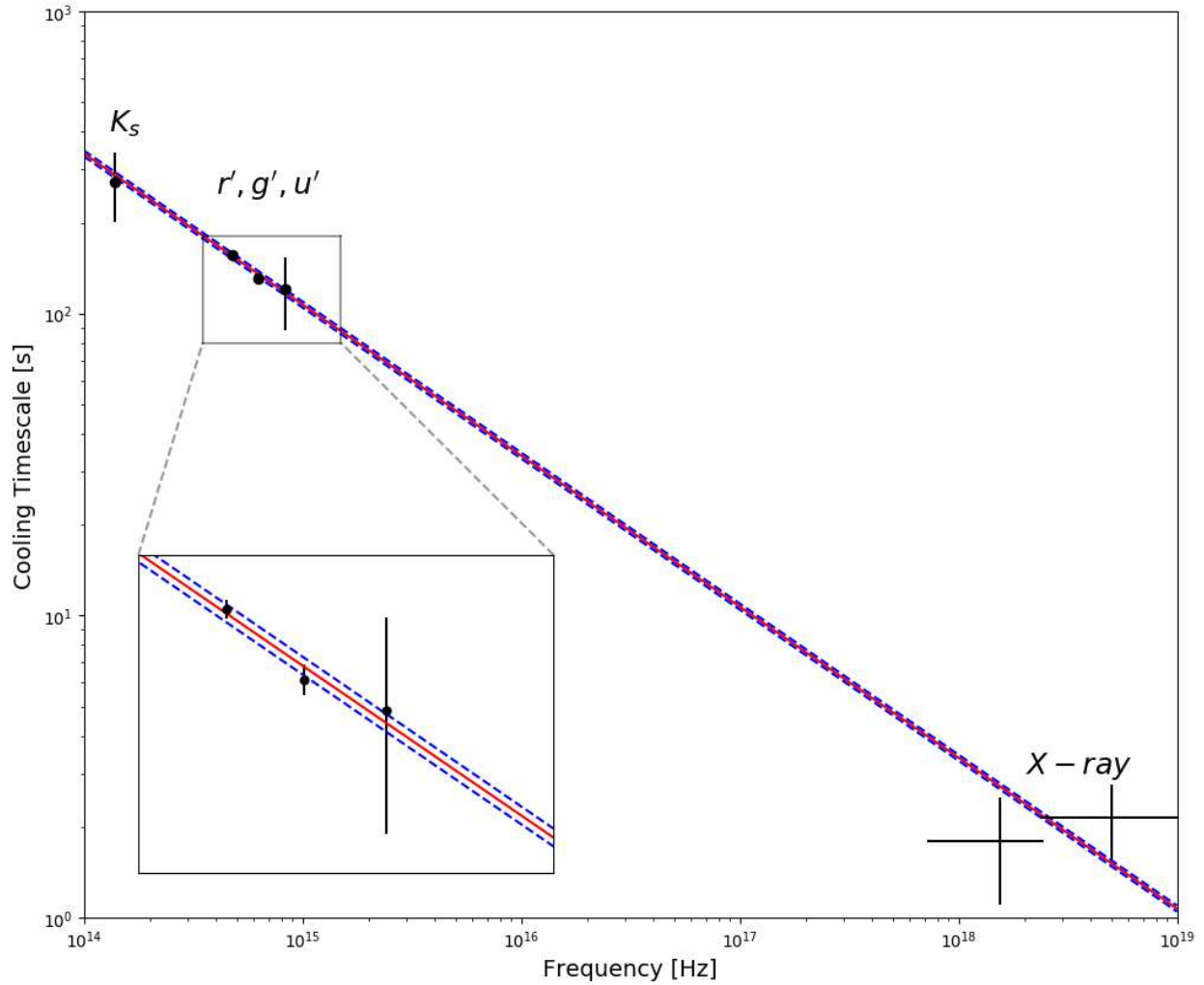
Fig. 3. Cooling timescale as a function of observed radiation frequency from near-IR to X-rays. The solid red line shows the best-fit single-zone magnetic field strength of 461 G, with dashed lines at ±12 G uncertainty. Note the excellent fit over 5 orders of magnitude in frequency with a reduced $\chi_\nu^2 = 0.8$ and a power-law dependence of $\tau \sim \nu^{-0.49 \pm 0.03}$, matching the $\nu^{-1/2}$ expectation for synchrotron cooling.
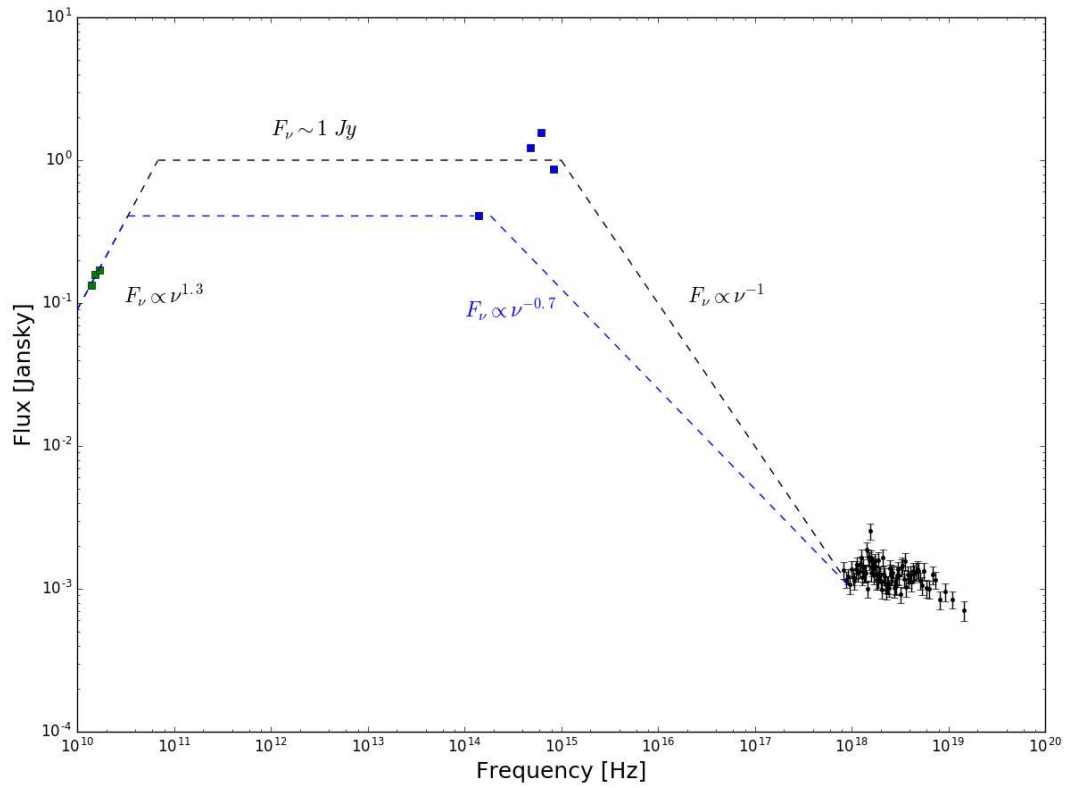
Fig. 4. Spectral energy distribution of the excess emission before the decay event (17).
Green: radio, blue: OIR, black: X-ray. We present approximate spectral slopes (dashed lines
connecting different energy regimes) as a rough guide to the slopes of apparent spectral breaks.

.
Table 1. Exponential decay timescales and magnetic field measurements..

Filter	Frequency (Hz)	Timescale (s)	Inferred Magnetic Field (G)
Ks	1.39×10^{14}	272 ± 70	479 ± 82
r'	4.76×10^{14}	157 ± 4	458 ± 7
g'	6.25×10^{14}	131 ± 5	472 ± 12
u'	8.33×10^{14}	121 ± 33	452 ± 81
X-ray (Soft)	1.55×10^{18}	1.8 ± 0.7	607 ± 157
X-ray (Hard)	5.03×10^{18}	2.2 ± 0.6	364 ± 68

Supplementary Materials:

Materials and Methods

Figures S1-S3

References (26-35)